Notes on Instability Thresholds in Solar Wind Plasma
Papers by Bale 2009, Kasper 2002, Hellinger 2006
M. Brown

Background: The solar wind plasma is essentially collision-less with the Coulomb mean-free-path about 1 AU. In addition, since the magnetic field drops with solar distance, and since the magnetic moment, $\mu = W_\perp/B$, is conserved, we expect temperature anisotropies to develop. In particular, since B drops, $T_\perp$ also has to drop. But since energy is conserved, energy is transferred to the parallel direction. Nonetheless, the mean proton temperature anisotropy at 1 AU is nearly unity: $T_\perp/T_\parallel = 0.89$, indicating that some process other than Coulomb collisions regulates temperature isotropy.

The idea of these three papers, and 100's of other related ones, is a statistical study of 1,026,112 parcels of solar wind plasma at 1 AU. Each parcel is 3 seconds in duration, so if the parcel is flowing at 400 km/s, the parcel is 1200 km in length. Typical proton gyro-radius is $\rho \leq 100$ km, and typical gyro period is ≤ 10 s. Measured quantities for each parcel include solar wind speed v_{SW}, density n, magnetic field $\mathbf{B}$ (including $\delta B_\parallel$ and $\delta B_\perp$), and both components of proton temperature, $T_\perp$ and $T_\parallel$. The key assumption is that the proton distributions are thermal bi-Maxwellians. This allows for simple models for kinetic instability thresholds using linear Vlasov theory. If we want to consider beams and sloshing ions, instability thresholds have to be carefully recalculated.

The main finding is that these 10^6 parcels of plasma are sharply bounded in a phase space $(T_\perp/T_\parallel, \beta_\parallel)$ by a number of kinetic instabilities. In other words, we never see very high or very low anisotropy at modest β. A simple model for the instability boundary, assuming a growth rate at marginal stability of $\gamma = 10^{-3}\omega_{ci}$ is given by:

$$\frac{T_\perp}{T_\parallel} = 1 + \frac{a}{(\beta_\parallel - \beta_0)^b}$$

where (see Figure below):

Instability	a	b	β_0
AIC	0.43	0.42	-0.0004
mirror	0.77	0.76	-0.016
par firehose	-0.47	0.53	0.59
obl firehose	-1.4	1.0	-0.1

Kasper, et al, GRL (2002): This was the discovery paper by Justin Kasper as part of his PhD thesis at MIT. He had the very clever idea to

generate a 2D histogram of many measurements of temperature anisotropy as a function of $\beta_\parallel = 2\mu_0 nkT_\parallel/B^2$, and compare to kinetic instabilities. In this GRL, Kasper studies the firehose instability as a constraint to the data. Sample distribution functions for $v_\parallel$ and $v_\perp$ are presented in his Figure 1, and the 2D proton histogram for $T_\parallel \geq T_\perp$ is the main result of the paper in his Figure 2.

Hellinger, et al, GRL (2006): This was a nice follow-on paper to the Kasper GRL adding the Alfvén ion cyclotron (AIC), mirror, parallel firehose, and oblique firehose instability thresholds to constrain the data. The main result is their Figure 2 showing that the $(T_\perp/T_\parallel, \beta_\parallel)$ histogram data is best bounded by mirror instability from above, and from the oblique firehose from below.

Bale, et al, PRL (2009): This is a highly cited culmination of ideas presented in the earlier papers by Stuart Bale (and Justin Kasper as co-author). It's a tour-de-force paper with several results. First, Bale confirms the Hellinger result that the that the $(T_\perp/T_\parallel, \beta_\parallel)$ histogram data is best bounded by mirror instability from above, and from the oblique firehose from below. In Figure 2 he shows that the AIC is not the instability threshold from above. That point is relevant for WHAM.

Figure 1 contains a lot of information. The top panel shows the full histogram with 10^6 independent measurements. The second panel shows that the fluctuation amplitude $\langle \delta B \rangle / \langle B \rangle$ for each measurement is enhanced at the instability boundaries. The third panel shows that the magnetic compressibility $\delta B_\parallel^2/(\delta B_\parallel^2 + \delta B_\perp^2)$ is enhanced at the upper firehose instability boundary at high $\beta_\parallel$.

The last panel of Figure 1 shows the "collisional age" of each parcel of plasma in the 2D histogram. The collisional age is the (dimensionless) number of Coulomb collisions suffered by a particular parcel since it left the surface of the Sun: $\tau \equiv \nu_{pp} L/V_{SW}$ where $L = 1AU$ and v_{SW} is the measured speed of the parcel at 1 AU. Of course all the parcels are measured at the same place (1 AU), but some are dense and moving in a slow packet, so have suffered many collisions in transit. Others are in a fast moving, low density, warm packet, so don't collide at all. The satisfying result is that collisionally old plasma is isotropic.

Figure 3 shows a histogram of the magnetic fluctuation amplitude $(\delta B)^2$ versus collisional age. We see that older plasma is more isotropic and therefore far from stability thresholds. Fluctuations fall off like $\tau^{-1/2}$. Finally, Figure 4 shows fluctuation spectra for the data. We see that around $k\rho_i \sim 1$, the spectra vary like $k^{-5/3}$.

CGL equations: One model for a kinetic plasma are the CGL equations. Note that these are the high density, low $B-$field limit of Jan Egedal's equations of state:

$$\frac{d}{dt}\left(\frac{P_\perp}{nB}\right) = 0$$

$$\frac{d}{dt}\left(\frac{P_\parallel B^2}{n^3}\right) = 0$$

These come from the first two adiabatic invariants. The first one comes from: $\mu = \frac{W_\perp}{B} = const$. The second one comes from the square of the flux in a tube of length L and particle number $N = nAL$: $\Phi^2 = B^2A^2 = \frac{B^2N^2}{n^2L^2}$. Now we notice that since $P_\parallel = nW_\parallel$ and $W_\parallel \sim v_\parallel^2$, if we use the second adiabatic invariant: $v_\parallel L = const$, we find that $W_\parallel \sim 1/L^2$ and $P_\parallel \sim n/L^2$. So our flux equation becomes:

$$\Phi^2 = \frac{B^2N^2}{n^2L^2} \sim \frac{B^2}{n^3}\frac{n}{L^2} \sim \left(\frac{P_\parallel B^2}{n^3}\right) = const$$

Since a spherical shell of solar wind increases in volume like r^2, we might expect the density to drop like r^{-2} (it does). If the magnetic field also drops like r^{-2} (or faster), the CGL equations predict (divide one by the other):

$$\frac{T_\perp n^2}{T_\parallel B^3} = const \rightarrow \frac{T_\perp}{T_\parallel} \sim \frac{B^3}{n^2} = r^{-2}$$

or that the solar wind should be dominated by $T_\parallel$. What's measured is isotropy. It turns out experimentally that the solar wind parameters fall off like: $n \sim r^{-2}, B_r \sim r^{-4}, T \sim r^{-1/2}$. The mean solar wind speed is pretty constant at 400 km/s after accelerating the first 10 R_{sun}.

The last expression is interesting. If the solar wind simply expanded and cooled adiabatically, then PV^γ and $TV^{\gamma-1}$ would be constant. Since a spherical shell of solar wind increases in volume like r^2, the adiabatic relation tells us $Tr^{2(\gamma-1)}$ is also a constant. If we use an adiabatic index of $\gamma = 5/3$, then the solar wind should cool like $T \sim r^{-4/3}$. The best fit Voyager measurements out to 20 AU shows $T \sim r^{-1/2}$. The implication is that turbulence takes magnetic energy to heat the plasma as it expands.

References:

S. D. Bale, et al., Magnetic Fluctuation Power Near Proton Temperature Anisotropy Instability Thresholds in the Solar Wind, Phys. Rev. Lett. **103**, (2009).

J. Egedal, et al., A review of pressure anisotropy caused by electron trapping in collisionless plasma, and its implications for magnetic reconnection, Physics of Plasmas **20**, 061201 (2013).

P. Hellinger, et al., Solar wind proton temperature anisotropy: Linear theory and WIND/SWE observations, Geophys. Res. Lett. **33**, L09101 (2006).

J. C. Kasper, et al., Wind/SWE observations of firehose constraint on solar wind proton temperature anisotropy, Geophys. Res. Lett. **29**, 1839 (2002).

J. C. Kasper, et al. Solar Wind Electrons Alphas and Protons (SWEAP) Investigation: Design of the Solar Wind and Coronal Plasma Instrument Suite for Solar Probe Plus. Space Sci Rev **204**, 131 (2016).

D. Verscharen, K. G. Klein, and B. A. Maruca, The multi-scale nature of the solar wind. Living Rev Sol Phys **16**, 5 (2019).

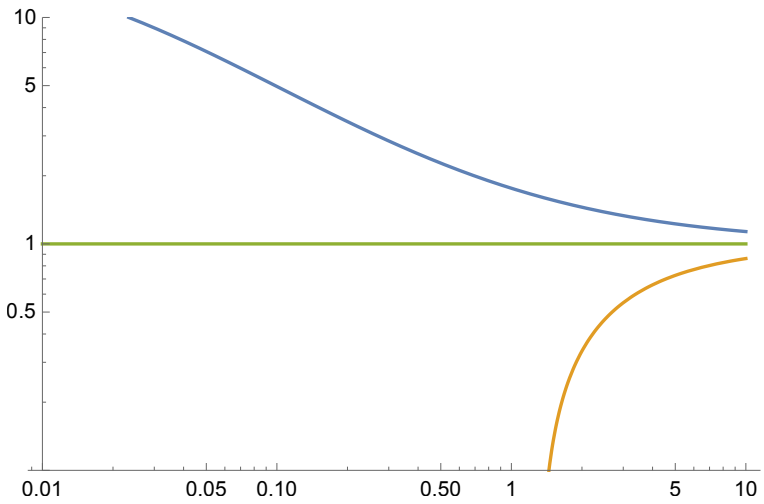

Figure 1: Brazil plot for mirror (above) and oblique firehose (below) instabilities. Horizontal axis is $\beta_\parallel$ and vertical axis is the temperature anisotropy $\frac{T_\perp}{T_\parallel}$. Note that for $\beta < 1$, there is essentially no instability limit for high $T_\parallel$, ie low $T_\perp/T_\parallel$. Also note that for WHAM, we will likely have non-thermal distributions of ion, not a simple bi-Maxwellian.